Journal of Applied Polymer Science

Fluorene-Based Click Polymers: Relationship Between Molecular Structure and Nonlinear Optical Properties

Xiaoli Ji,[1,2] Shanyi Guang,[1] Hongyao Xu,[1] Fuyou Ke,[1] Xiaoyun Qin[1]

[1]College of Material Science and Engineering & State Key Laboratory for Modification of Chemical Fibers and Polymer Materials, Donghua University, Shanghai 201620, China

[2]Department of Chemical Engineering, Anhui University of Science and Technology, Huainan 232001, China

Correspondence to: H. Xu (E-mail: hongyaoxu@163.com)

ABSTRACT: To further understand the relationship between the polymer structure and nonlinear optical (NLO) property, in this article, three fluorene-based triazole functional polymers with different linked chains were designed and controllably prepared by click chemistry method. The structures and properties of these polymers were characterized and evaluated with Fourier transform infrared spectroscopy, nuclear magnetic resonance spectroscopy, ultraviolet spectroscopy, fluorescence spectra, dynamic state laser light scattering, thermogravimetric analysis, and NLO analyses. The results exhibited that the target polymers displayed good solubility, high thermal stability, and well NLO properties. The relationships between molecular structures and optical properties were investigated by both theoretical simulation and experimental results. It was found that the rigid conjugated linked chain between triazole and chromophore can effectively enhance the NLO properties of the resultant polymers. The suitable rigid and flexible groups in the triazole polymers will result in good thermal stabilities. © 2014 Wiley Periodicals, Inc. J. Appl. Polym. Sci. **2014**, *131*, 40878.

KEYWORDS: optical properties; properties and characterization; structure-property relations

Received 17 October 2013; accepted 21 April 2014

DOI: 10.1002/app.40878

INTRODUCTION

With the rapid development of laser technology, many nonlinear optical (NLO) materials with large third-order nonlinearity have been prepared and their application for optical communication, optical limiting, optical data storage, and information processing were investigated.[1,2] Among all these materials identified, organic NLO materials such as azobenzene derivatives,[3,4] polyarylenes,[5] polyacetylenes (PAs),[6,7] and organometallic complex,[8,9] have attracted great interest owing to high third-order optical nonlinearities.

In the past years, our group also mainly focused on molecular design and relationship between the molecular structures and their properties of functional PA with large NLO susceptivity.[10–16] A series of PAs containing azobenzene or stilbene derivatives were designed, and the effects of different pendant structures such as different conjugation length, conjugation bridge structure, and jointed group structure on their optical properties were investigated. It was found that functional PAs possessed significantly enhanced thermal stability owing to the "jacket effect" of aromatic azobenzene pendants. Similar phenomenon was also observed in PAs-containing oxadiazole heterocyclic ring.[17–19]

The discovery of "click chemistry" has brought a new revolution for controllably preparing NLO materials for its remarkable features, such as simple operation, high yield, easy product postprocessing, and insensitivity to water and oxygen.[20–22] The electron-poor heterocycle named triazole unit can be readily synthesized in this efficient way and can significantly enhance the thermal stability of the resultant materials. Now, triazole-based functional polymers involving NLO materials[23,24] have been prepared by click chemistry; however, the influence of different linked chain structures in triazole-based polymers on NLO property of polytriazoles has been rarely reported.

Fluorene derivants is a kind of very important NLO chromophore for its many remarkable advantages[25,26] such as high β value, big band-gap energy, easily modifiable structure, etc. In this article, three fluorene-based polytriazoles with different linked triazole groups were designed and synthesized by click chemistry. The relationships between the linked triazole groups, NLO property, and influence of molecular structure on thermal and optical properties of the resultant polymers were investigated in detail.

EXPERIMENTAL

Materials

Unless otherwise noted, all commercial reagents were used as received. 2-Methyl-3-butyne-2-ol, 1,4-dibromobenzene, and 1,4-

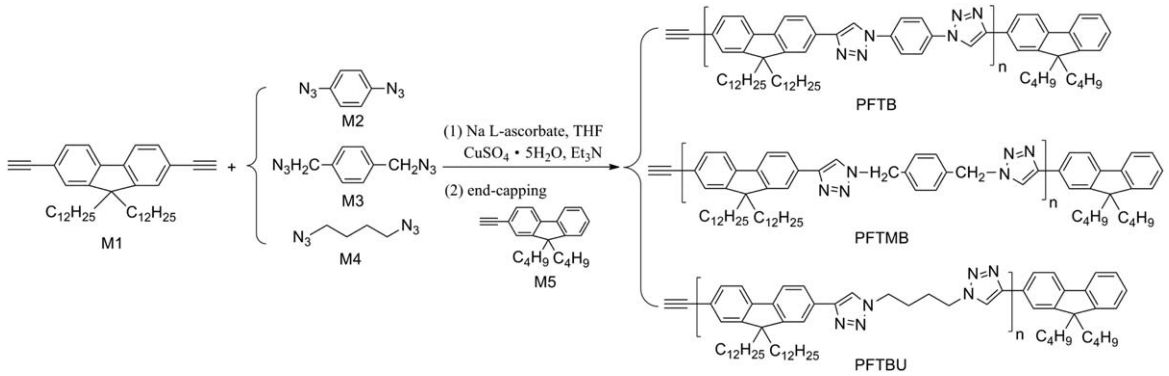

Scheme 1. The synthetic procedures of the target fluorene-based click polymers.

dibromobenzyl were obtained from ACROS International Ltd. Bis(triphenylphosphine)palladium(II) chloride [$PdCl_2(PPh_3)_2$] was purchased from Aldrich (St. Louis, MO). 2,7-Dibromofluorene, 2-bromofluorene, 1,4-dibromobutane, tetrabutyl ammonium bromide, sodium azide, cuprous iodide, anhydrous ethyl alcohol, methanol, NaOH, $MgSO_4$, dichloromethane, petroleum ether, and ethyl acetate were all purchased from Shanghai Chemical Reagent Company. Dioxane and tetrahydrofuran (THF) were distilled from sodium benzophenone ketyl immediately prior to use. Triethylamine (TEA) was distilled from potassium hydroxide prior to use.

Instruments

Fourier transform infrared (FTIR) spectra of KBr disks were measured with a Nicolet NEXUS 870 FTIR spectrophotometer at room temperature; 32 scans were collected at a resolution of 1 cm^{-1}. ^1H nuclear magnetic resonance (NMR) (400 MHz) spectra were recorded on a Bruker DMX-500 spectrometer using tetramethylsilane (0.00 ppm) as the internal standard in chloroform-d ($CDCl_3$) at room temperature. Weight–average (M_w) molecular weights were determined by BI-200SM static/dynamic state laser light scattering instrument at 30°C. THF was used as the solvent. Thermogravimetric analysis was carried out using a TGA 2050 thermogravimetric analyzer with a heating rate of 10°C/min from 30°C to 700°C under a continuous nitrogen purge (100 mL/min). Samples (15–25 mg) were loaded in alumina pans. The thermal degradation temperature (T_d) was defined as the temperature of 5% mass loss. Ultraviolet (UV) spectra of the polymers were investigated in THF (ca. 1×10^{-5} M) at room temperature in 1 cm quartz cell using a Shimadzu UV-265 spectrometer. Fluorescence spectra were obtained on a Shimadzu RF-5301PC spectrofluorimeter equipped with a 450-W Xe lamp and a time-correlated single-photon counting card. The NLO properties of the samples were performed by open and close aperture Z-scan technique with a frequency doubled, Q-switched, mode-locked continuum ns/ps Nd : YAG laser system, which provides linearly polarized 4 ns optical pulses at 532 nm wavelength with a repetition of 1 Hz. The experiment was set up as in the literature.[27] The spatial distribution of the pulse was nearly a Gaussian profile. The THF solution of the polymer (concentration: $c = 0.005M$) was contained in a quartz cell with a thickness of 2 mm. The reference sample ZnSe used in this article was 2 mm thick and was polished to avoid light scattering. It was a single crystal, and its linear refraction index was 2.4. The linear transmittance of ZnSe was measured to be 59%. The samples were placed on a translation stage controlled by a computer and moved along the z-axis with respect to the focal point of a 300-mm focal lens. The input energy was 15 μJ. The radius ω_0 at beam waist was 25 mm. The input laser pulses adjusted by an attenuator (Newport) were split into two beams. The two beams were simultaneously measured by using two energy detectors, D1 and D2 (Rjp-735 energy probes, Laser Precision). One was used as a reference to monitor the incident laser energy, and the other was focused on the sample cell.

Monomer Synthesis

The structures of the five monomers 2,7-diethynyl-9,9-didodecylfluorene (M1), 1,4-diazido-benzene (M2), 1,4-diazido-benzyl (M3), 1,4-diazido-tetrane (M4), and 2-ethynyl-9,9-dibutylfluorene (M5) are shown in Scheme 1. 2,7-Diethynyl-9,9-didodecylfluorene (M1) was synthesized through the intermediate products of 2,7-dibromo-9,9-didodecylfluorene (1) and 2,7-(2-methyl-3-butyne-2-ol)−9,9-didodecylfluorene (2) using a slight modification of the method reported in the literature.[28]

2,7-Dibromo-9,9-didodecylfluorene (1). 2,7-Dibromofluorene (3.88 g,12 mmol) and tetrabutyl ammonium bromide (22.5 mg, 0.1 mmol) were dissolved in 50 mL dimethyl sulfoxide. After the reaction mixture was stirred violently, 4 mL of 0.5M aqueous NaOH solution and 1-bromododecane (7.0 mL, 29 mmol) were added drop wise to the mixture. The reaction mixture was stirred at room temperature for 3 h, and then was extracted with CH_2Cl_2. The organic phase was purified by column chromatography on silica gel with petroleum ether to white crystal (90.3%). IR (KBr), ν (cm^{-1}): 2956, 2920 (CH_3), 2850 (CH_2), 1597, 879 (Ar). ^1H NMR (400 MHz, $CDCl_3$, δ): 7.52 (d, $J = 7.7$, 2H; Ar H), 7.45 (m, 4H, Ar H), 1.92 (m, 4H, CH_2), 1.28–1.04(m, 36H, CH_2), 0.88 (t, $J = 7.2$, 6H; CH_3), 0.59 (m, $J = 4.0$, 4H; CH_2).

2,7-(2-Methyl-3-butyne-2-ol)-9,9-didodecylfluorene (2). Under nitrogen, a mixture of the compounds 2,7-dibromo-9,9-didodecylfluorene (3.30 g, 5.0 mmol), 2-methyl-3-butyne-2-ol (4 mL, 40 mmol), $PdCl_2(PPh_3)_2$ (175 mg, 0.25 mmol), and CuI (50 mg, 0.25 mmol) was dissolved in 30 mL TEA and 30 mL THF. The reaction mixture was refluxed at 70°C for 48 h. After cooling to room temperature, the insoluble particles were filtered off. After the removal of the solvent with a rotary evaporator, water and CH_2Cl_2 were added to the mixture, and the organic

Table I. M_w and Solubility of the Target Fluorene-Based Click Polymers

Samples	M_w (Da)	THF	CH_2Cl_2	DMF	DMSO	Methanol
PFTB	4,717	++	++	+	+	-
PFTMB	35,642	++	++	+	+	-
PFTBU	84,508	++	++	+	+	-

(++): soluble; (+): slightly soluble; (-): not soluble.

phase was purified by column chromatography on silica gel with ethyl acetate/petroleum ether mixture (1 : 2 v/v) to give yellow powder (68.1%). IR (KBr), ν (cm^{-1}): 3309 (C≡C—H), 2920 (CH_3), 2853 (CH_2), 2106 (RC≡CH), 1639 (Ar), 887 (Ar). ^{1}H NMR (400 MHz, $CDCl_3$, δ): 7.60 (d, J = 7.7, 2H; Ar H), 7.38 (m, 4H, Ar H), 2.03 (s, 2H, OH), 1.92 (m, 4H, CH_2), 1.27–1.02 (m, 36H, CH_2), 0.87 (t, J = 7.2, 6H; CH_3), 1.65 (s, 12H, CH_3), 0.54 (m, J = 4.0, 4H; CH_2).

2,7-Diethynyl-9,9-didodecylfluorene (M1). Under nitrogen, a mixture of 2,7-(2-methyl-3-butyne-2-ol)-9,9-didodecylfluorene (0.333 g, 0.5 mmol) and NaOH (0.2 g, 5.0 mmol) was added into 20 mL 1,4-dioxane. The reaction mixture was refluxed at 80°C for 8 h. After cooling to room temperature, water and CH_2Cl_2 were added to the mixture, and the organic phase was purified by column chromatography on silica gel with petroleum ether to give white powder (89.5%). IR (KBr), ν (cm^{-1}): 3309 (C≡C—H), 2920 (CH_3), 2853 (CH_2), 2106 (RC≡C—H), 1639 (Ar), 887 (Ar). ^{1}H NMR(400 MHz, $CDCl_3$, δ): 7.62 (d, J = 7.6, 2H; Ar H), 7.46 (t, J = 5.6, 4H; Ar H), 3.13 (s, 2H, C≡C—H), 1.93 (m, 4H, CH_2), 1.27–1.02 (m, 36H, CH_2), 0.86 (t, J = 6.9, 6H; CH_3), 0.57 (d, J = 7.2, 4H; CH_2). Anal. Calcd. for $C_{41}H_{58}$: C 89.39, H 10.61; Found: C 89.13, H 10.79.

1,4-Diazido-benzene (M2). Under nitrogen, 1,4-dibromobenzene (1.18 g, 5 mmol), NaN_3 (1.3 g, 20 mmol), CuI (0.19 g, 1.0 mmol), L-proline (0.345 g, 3.0 mmol), and (0.12 g, 3.0 mmol) NaOH were dissolved in THF/H_2O (10 mL, 7 : 3). The mixture was stirred at 95°C for 24 h. After cooling to room temperature, water and ethyl acetate were added to the mixture, and the organic phase was purified by column chromatography on silica gel with petroleum ether to give yellow powder (61.0%). IR (KBr), ν (cm^{-1}): 2102 (N_3), 1500 (Ar), 832 (Ar). ^{1}H NMR (400 MHz, $CDCl_3$, δ): 7.01 (s, 4H, Ar H). Anal. Calcd. for $C_6H_4N_6$: C 45.00, H 2.52, N 52.48; Found: C 44.81, H 2.74, N 52.56.

1,4-Diazido-benzyl (M3). Under nitrogen, a mixture of 1,4-dibromobenzyl (2.64 g, 10 mmol) and NaN_3 (2.60 g, 20 mmol) was added into 20 mL dimethylformamide. The reaction mixture was refluxed at 50°C for 4 h. After cooling to room temperature, water and CH_2Cl_2 were added to the mixture, and the organic phase was purified by column chromatography on silica gel with petroleum ether to give white powder (90.0%). IR (KBr), ν (cm^{-1}): 2930 (CH_2), 2860 (CH_2), 2100 (N_3), 1515 (Ar), 1442 (Ar), 816 (Ar). ^{1}H NMR (400 MHz, $CDCl_3$, δ): 7.35 (s, 4H, Ar H), 4.36 (s, 4H, CH_2). Anal. Calcd. for $C_8H_8N_6$: C 51.06, H 4.28, N 44.66; Found: C 50.92, H 4.53, N 44.82.

1,4-Diazido-tetrane (M4). This was prepared as M3 above. Yellow oil (85.0%). IR (KBr), ν (cm^{-1}): 2945 (CH_2), 2874 (CH_2), 2098 (N_3). ^{1}H NMR (400 MHz, $CDCl_3$, δ): 3.26 (m, 4H, CH_2), 1.61 (m, 4H, CH_2). Anal. Calcd. for $C_4H_8N_6$: C 34.28, H 5.75, N 59.97; Found: C 34.14, H 5.88, N 60.18.

2-Ethynyl-9,9-dibutyl fluorene (M5). This was prepared as M1 above. Yellow oil (92.0%). IR (KBr), ν (cm^{-1}): 3278 (C≡C—H), 2955 (CH_3), 2929 (CH_3), 2863 (CH_2), 2100 (RC≡C—H), 1600 (Ar), 887 (Ar). ^{1}H NMR (400 MHz, $CDCl_3$, δ): 7.64 (m, 2H, Ar H), 7.48 (t, J = 4.5, 3H; Ar H), δ7.34 (m, 2H, Ar H), δ3.13 (s, 1H, C≡C—H), δ1.96 (t, J = 8.3, 4H; CH_2), δ1.06 (m, 8H, CH_2), δ0.68 (t, J = 7.4, 6H; CH_3). Anal. Calcd. for $C_{23}H_{26}$: C 91.34, H 8.66; Found: C 91.16, H 8.79.

Polymerization

The structures of the three target polymers PFTB, PFTMB, and PFTBU are shown in Scheme 1.

Poly[fluorene-(1,2,3-triazol-4-yl)-1,4-phenylene] (PFTB). Diazide-(M2) and diethynyl-based monomers (M1) (1 : 1 equiv, 0.32 mmol of each), sodium L-ascorbate (10 mol%), and $CuSO_4{\cdot}5H_2O$ (5 mol%) were dissolved in THF (2–3 mL) under N_2 flow in a flame-dried Schlenk flask, and TEA (0.2–0.3 mL) was added to the mixture as a ligand. The mixture was stirred at 45°C for 48 h. Then, a spot of M5 as the capping agent was put into the reaction system and went on for 2 h. The mixture was washed with an ethylenediaminetetraacetic acid-saturated solution followed by water. The organic layer was separated, and the solvent was removed. The resulting polymer was obtained by precipitating into methanol. Then, the resultant was dissolved in THF and precipitated in methanol three times for purification. To improve the purity of the polymer, the precipitated polymer was further purified by multiple Soxhlet extraction with methanol, hexane, and finally extracted with chloroform. The product was dried in vacuum oven at 60°C to give brown powder (211.0 mg, 92.0%): IR (KBr), ν (cm^{-1}): 3310 (C≡C—H), 2926 (CH_3), 2853 (CH_2), 2103 (RC≡CH), 1620 (triazole), 1524 (Ar), 890 (Ar). ^{1}H NMR(400 MHz, $CDCl_3$, δ): 8.35 (s), 7.98–8.07 (m, Ar H), 7.77–7.91 (m, triazole H), 7.67–7.68 (m, Ar H), 7.49–7.51 (m, Ar H), 3.16 (s, C≡C—H), 2.02–2.04 (d, CH_2), 1.05–1.25 (m, CH_2), 0.81–0.86 (m, CH_3), 0.63–0.69 (d, CH_2).

Poly[fluorene-(1,2,3-triazol-4-yl)-1,4-benzyl] (PFTMB). This was prepared as PFTB above. Yellow powder (86.9%): IR (KBr), ν (cm^{-1}): 2923 (CH_3), 2850 (CH_2), 1613 (triazole), 1514 (Ar), 890 (Ar). ^{1}H NMR (400 MHz, $CDCl_3$, δ): 7.86 (s, triazole H), 7.72 (s, Ar H), 7.64 (s, Ar H), 7.33 (s, Ar H), 7.22 (s, Ar H), 5.57 (s,CH_2), 1.98 (s,CH_2), 1.57–0.95 (m,CH_2), 0.80 (s,CH_3), 0.56 (s, CH_2).

Poly[fluorene-(1,2,3-triazol-4-yl)-1,4-tetrane] (PFTBU). This was prepared as PFTB above. Yellow powder (90.1%): IR (KBr), ν (cm^{-1}): 2924 (CH_3), 2851 (CH_2), 2103 (RC≡CH), 1613

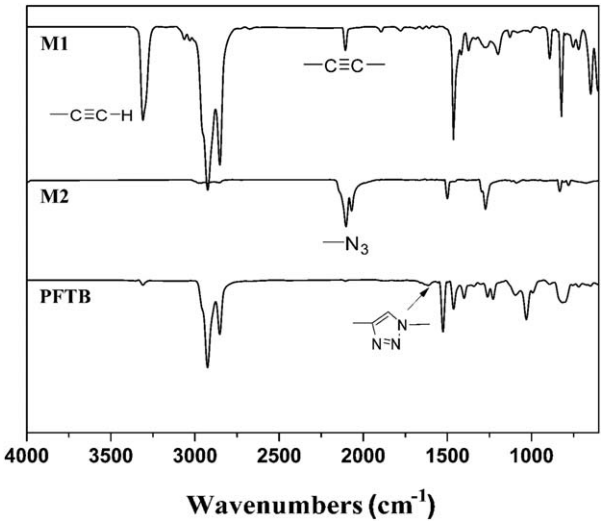

Figure 1. The FTIR spectra of M1, M2, and the target fluorene-based click polymer PFTB.

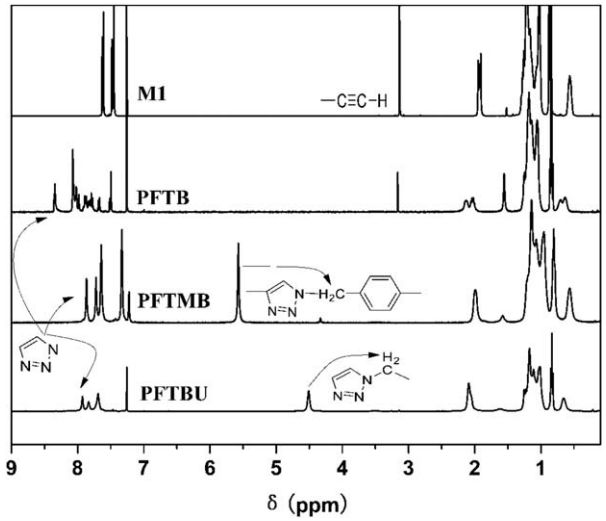

Figure 2. The ^{1}H NMR spectra of M1 and the target fluorene-based click polymers.

(triazole). ^{1}H NMR (400 MHz, $CDCl_3$, δ): 7.92 (s, triazole H), 7.83 (s, Ar H), 7.69 (s, Ar H), 4.51 (s, CH_2), 2.09 (s,CH_2), 1.01–1.25 (s,CH_2), 0.81–0.85 (s,CH_3), 0.66 (s,CH_2).

RESULTS AND DISCUSSION

Scheme 1 illustrates the synthetic procedures of the target fluorene-based click polymers. The designed 1,4-disubstituted 1,2,3-triazole ring units were introduced into the fluorene-based polymer backbone using different 1,4-diazido monomers by click coupling with 2,7-diethynyl-9,9-didodecylfluorene at a 1 : 1 mole ratio, and 2-ethynyl-9,9-dibutyl fluorene was used as an end-capping monomer. Table I shows the M_w of three triazole polymers. The M_w of the polymers PFTB, PFTMB, and PFTBU were 4717, 35,642, and 84,508, respectively. The M_w shows very large difference though they were synthetized in the same condition, which was ascribed to the larger steric hindrance of monomer M2 (1,4-diazido-benzene) compared with those of M3 and M4. The rigid conjugated structure results in large molecular tensile force, which will go against formation of high polymer. That is, the smaller steric hindrance the diazido monomer has, the easilier the click reaction happens, then the larger M_w the corresponding product has.

The solubility of three triazole polymers was also investigated, and the results are listed in Table I. All the polymers possess good solubility in common solvents such as THF, CH_2Cl_2, dimethylformamide, and dimethyl sulfoxide, except methanol. The reason may be from the fact that the long alkyl chains of fluorene monomer have endowed the resultant polymers with good solubility, though many rigid rings like fluorene rings, triazole rings, and benzene rings are incorporated.

Structural Characterization

The structures of the three resultant polymers were characterized by spectroscopic techniques. FTIR spectra of M1, M2, and PFTB are shown in Figure 1. It can be seen that M1 exhibits a strong characteristic absorption band at ca. 3309 and 2106 cm^{-1}, corresponding to the C—H stretching vibration in the disubstituted acetylene molecules and C≡C stretching vibration, respectively. M2 exhibits a strong characteristic absorption band near 2103 cm^{-1}, due to the azide stretching vibration. For PFTB, a strong characteristic absorption band at 1620 cm^{-1} attributed to triazole emerges, accompanying with the disappearance of the characteristic υ_s (≡C—H) absorption band and the azide stretching vibration υ_s ($^{-}$N≡N^{+} absorption band), which confirms that the triazol ring was formed.

Figure 2 shows the ^{1}H NMR spectra of M1 and three polymers. The characteristic absorption of the acetylene proton in M1 is located at 3.13 ppm as a singlet peak, but completely disappears in the spectrum of polymers PFTMB and PFTBU. Simultaneously, the characteristic absorptions at $\delta = 8.35$, 7.86, and 7.92 ppm attributed to the olefin proton of the triazole ring emerge in the spectra of three resultant polymers, respectively. In addition, the characteristic vibrations at $\delta = 5.57$ and 4.51 ppm appear in the spectra of PFTMB and PFTBU, respectively, which are attributed to the methylene proton between benzene ring and triazole ring of PFTMB and the methylene proton between alkyl chain and triazole ring of PFTBU, respectively. The characteristic absorptions of methylene proton have moved to low field mainly due to the conjugation effect between methylene and benzene ring and triazole ring; these are consistent with Ref. 29. These all prove that click reaction has taken place, and the triazole polymers have been produced.

Optical Properties

The photophysical properties of monomer M1 and polymers PFTB, PFTMB, and PFTBU were studied by UV–vis absorption and fluorescence emission spectra in THF solution. It can be seen from Figure 3 that monomer M1 displays UV absorption peaks at 302, 315, 321, and 329 nm, which corresponds to the π-π^* electronic transitions of the conjugated fluorene groups and acetylene groups. The UV absorption peaks of the resultant polymers display obvious red shift compared with that of monomer M1 owing to the conjugation effect in polymers. Simultaneously, it was also found out that the UV absorption

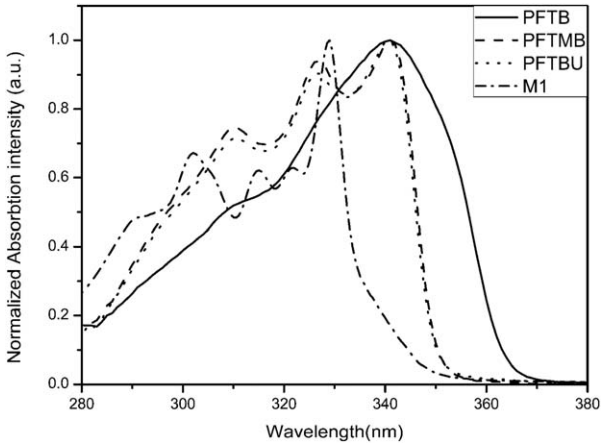

Figure 3. The normalized UV–vis absorption spectra of M1 and the target fluorene-based click polymers in THF.

peaks of polymer PFTB is only a broad peak at 341 nm, which is assigned to π-π^* electronic transitions of the fluorene groups, triazole groups, and benzene groups. The disappearance of fine structures' peaks may be owing to the linked rigid rings. PFTMB and PFTBU show the same absorption peaks at 310, 326, and 341 nm, which are mainly originated from π-π^* electronic transitions of the fluorene groups and triazole groups.

It is worth noting that the maximum UV absorption edge of PFTB is obvious red shift compared with the others. This may be the reason that the polymer PFTB has the π-electronic conjugation among fluorene rings, triazole rings, and benzene rings. The maximum UV absorption edge of PFTMB and PFTBU is at the similar position though there is a little n-π^* electronic transitions of the benzene groups and methylene in PFTMB.

Figure 4 shows the fluorescence emission spectra of M1, PFTB, PFTMB, and PFTBU in THF solution. As seen in Figure 4, the maximum fluorescence emission peaks of M1 and the three polymers are located at 361, 367, 366, and 366 nm, respectively. The maximum fluorescence emission peaks of the resultant polymers display obvious red shift compared with that of monomer M1, and the maximum fluorescence emission peaks

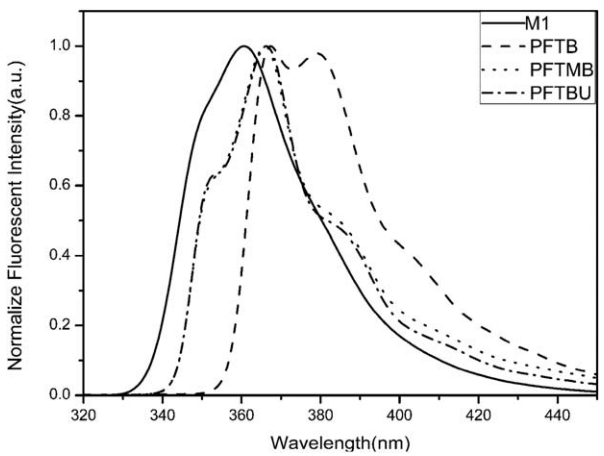

Figure 4. The normalized fluorescence emission spectra of M1 and the target fluorene-based click polymers in THF.

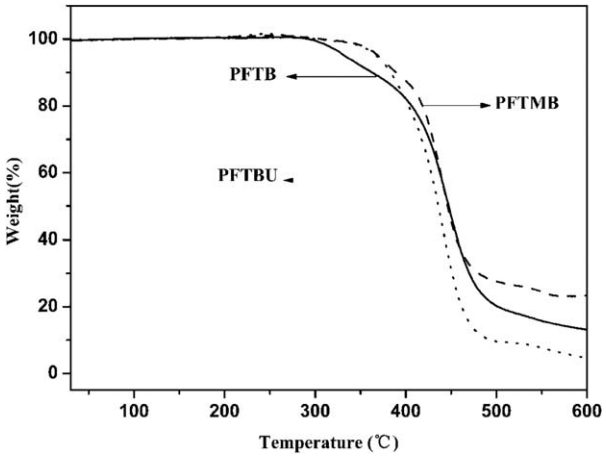

Figure 5. The thermogravimetric analysis spectra of the target fluorene-based click polymers.

of PFTMB and PFTBU exhibit at almost same position, whereas the fluorescence emission edge of PFTB shows greater red shift compared with the other two polymers. These phenomena are consistent with that of the UV absorption.

Thermal Analysis

As shown in Figure 5, the T_ds (weight loss 5%) of PFTB, PFTMB, and PFTBU were 333°C, 369°C, and 367°C, respectively, indicating that the incorporation of rigid triazole group into fluorene-based copolymers has endowed the polymers with high thermal stability. The polymer PFTB has the lowest T_d though it has the best rigid conjugated molecular structure. It may be the reason that rigid conjugated structure will result in larger tension in the process of molecular vibration and movement, which cause breakage of molecular chain at the lower temperature. When the alkyl chains were incorporated into molecular chain, the vibration tension of molecular chain decreased and thermal stability increased. It means that the incorporation of flexible chain can weaken the torsional vibration among rigid groups to prompt the improvement of thermal stability.

Structure Optimization and Theoretical Calculation

In order to elucidate the geometrical characteristics and molecular orbital energy level of the polytriazoles accurately, the full geometry was optimized using the B3LYP/6–31G level of theory implemented in the Gaussian 03 suite of program.[30–32] To simplify the calculations, the basic structural units of these two compounds were selected, and the bonds at the end of the structural units were saturated with hydrogen atoms. The results are shown in Figure 6 and Table II. It was found that the dihedral angles between the fluorene rings and triazole rings in the three polymers are all close to 180°; they are close to coplanar. Although the dihedral angle between the triazole ring and benzene ring in PFTB is 160.043°, the dihedral angles between the triazole ring and methylene in PFTMB and PFTBU are 104.651° and 98.196°, respectively, hinting that coplanarity decreases; this supports the relationships of their nonlinearity among the three resultant polymers. Correspondingly, the calculated molecular orbital energy level of PFTB was narrower compared with that

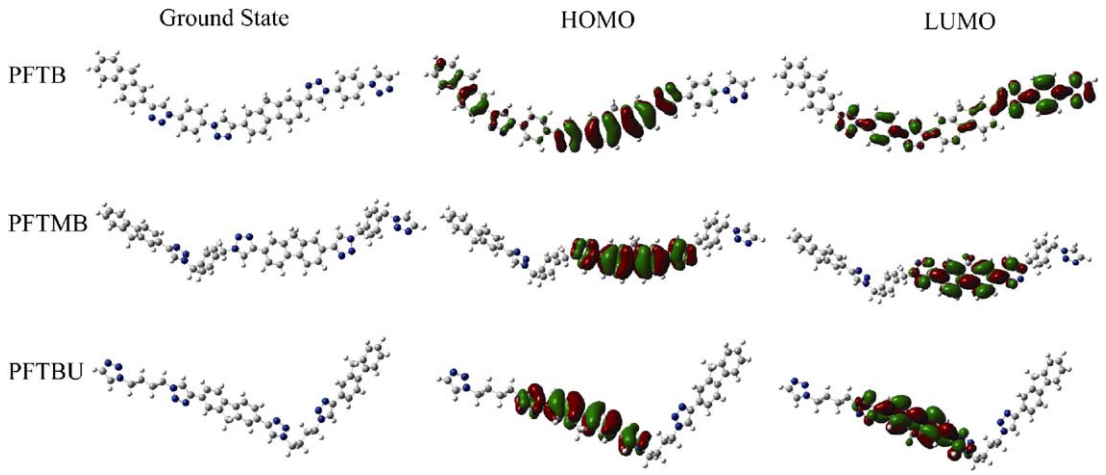

Figure 6. The optimized geometry of PFTB, PFTMB, PFTBU, C, N, and H atoms are represented as gray, blue, and white–gray, respectively. [Color figure can be viewed in the online issue, which is available at wileyonlinelibrary.com.]

of PFTMB and PFTBU, which is in accordance with the red shift of spectra. The calculated molecular orbital energy level of PFTMB and PFTBU are similar, which is in accordance with the similar position of their UV absorption and fluorescence emission peaks. It means that the rigid conjugated linked chain between triazole and chromophore will result in different conjugation, coplanarity, electronic transmission, and photophysical properties of the resultant polymers.

Nonlinear Absorption Properties

The nonlinear absorption behavior of the resultant polymers in THF was evaluated by the Z-scan technique under an open aperture configuration. In theory, the normalized transmittance for the open aperture configuration can be written as[27]:

$$T(z, s=1)=\sum_{m=0}^{\infty}\frac{[-q_0(Z)^m]}{(m+1)^{3/2}},\ \text{for}\ |q_0|<1 \qquad (1)$$

where s = 1 indicates no aperture, $q_0(Z) = \beta I_0(t) L_{eff}/(1 + Z^2/Z^2{}_0)$, β is the nonlinear absorption coefficient, $I_0(t)$ is the intensity of laser beam at focus ($z = 0$), $L_{eff} = [1 - \exp(-\alpha_0 L)]/\alpha_0$ is the effective thickness where α_0 is the linear absorption coefficient and L the sample thickness, z_0 is the diffraction length of the beam, and z is the sample position. The results from the Z-scan experiments are demonstrated in Figure 7. The solid lines in Figure 7 are theoretical curves from eq. (1).

The normalized transmission for the closed aperture Z-scan is given by[27]

$$T(z, \Delta\phi)=1+\frac{4\Delta\phi}{(x^2+9)(x^2+1)} \qquad (2)$$

where $x = Z/Z_0$ and $\Delta\phi$ is on-aixs phase change caused by the nonlinear refractive index of the sample and $\Delta\phi=2\pi I_0(1-e^{-\alpha_0 L})n_2/\lambda\alpha_0$. Thus, the nonlinear refractive coefficient of PFTB was determined to be 1.50×10^{-16} m^2/W, by fitting the experimental data using eq. (2).

The $\chi^{(3)}$ can be calculated by the following equation[6]:

$$\chi^{(3)}=\sqrt{\left|\frac{cn_0^2}{80\pi}n_2\right|^2+\left|\frac{9\times10^8\varepsilon_0 n_0^2 c^2}{4\pi\omega}\alpha_2\right|^2} \qquad (3)$$

where ε_0 is the permittivity of vacuum, c the speed of light, n_0 is the refractive index of the medium, and $\omega = c/2\pi\lambda$.

It can be seen in Figure 7 that the polymers have both nonlinear absorption and nonlinear refraction. Thus, the $\chi^{(3)}$ of the polymers should be dual attributed to nonlinear absorption and nonlinear refraction of the molecules. The data collected in Table III indicate that they all exhibit good nonlinear properties with effective $\chi^{(3)}$ values of 3.66×10^{-10} esu for PFTB, 1.96×10^{-10} esu for PFTMB, and 1.22×10^{-10} esu for PFTBU. In order to verify the reliability of the nonlinear parameters of these new polymers, the nonlinear properties of ZnSe, which

Table II. The Data of Theoretical Calculation Molecular Orbit

	Dihedral angles				
Polymers	Between fluorene and triazole rings	Between triazole and benzene rings (methylene)	HOMO	LUMO	E_g[c]
PFTB	179.068	160.043	−5.6081	−1.9497	3.6584
PFTMB	179.175	104.651	−5.4441	−1.2754	4.1690
PFTBU	179.059	98.196	−5.4656	−1.2964	4.1692

[a] E_g = LUMO − HOMO.

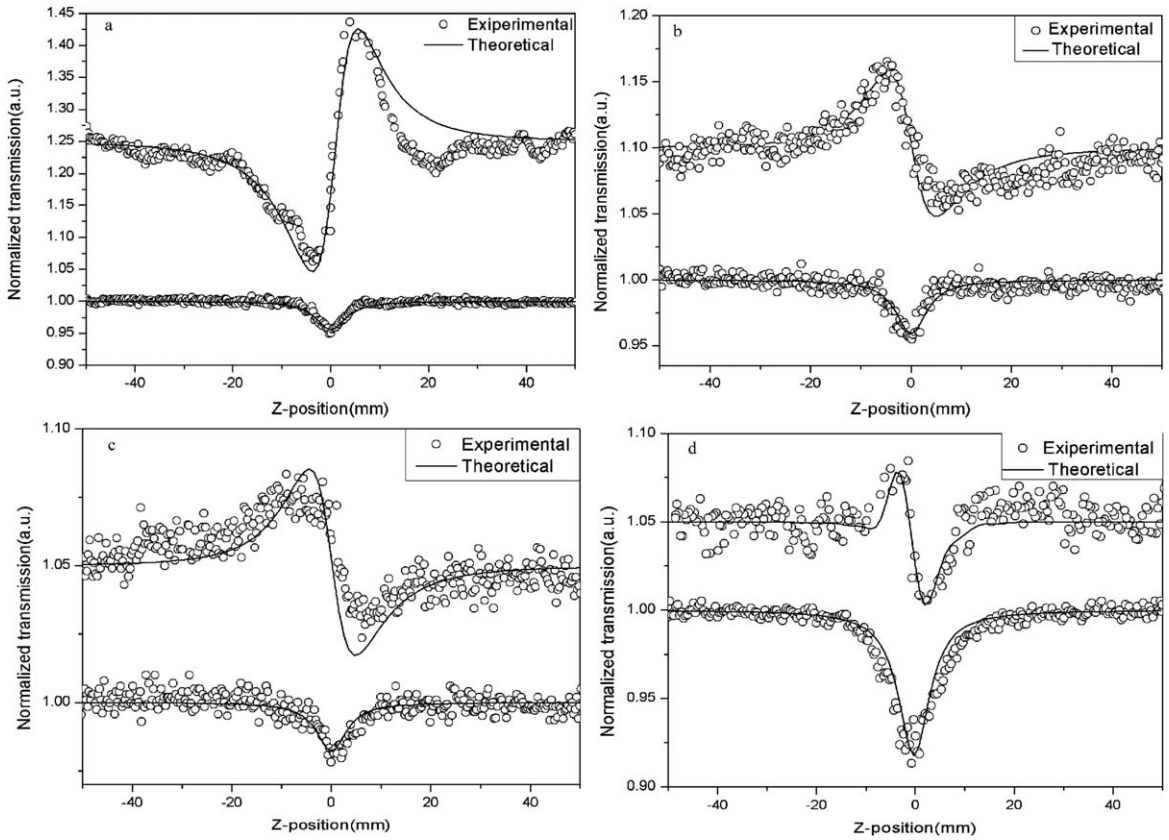

Figure 7. Normalized open-aperture (under) and close-aperture (upper) Z-scan transmittance of PFTB (a), PFTMB (b), and PFTBU (c). Dotted line: experimental data; solid line: theoretical curve. The curves have been vertically shifted for clarity. [Color figure can be viewed in the online issue, which is available at wileyonlinelibrary.com.]

has been extensively studied as NLO material, were also studied by open and close aperture Z-scan technique used for these polymers. From Table III it was found that the nonlinear absorption, nonlinear refraction, and effective $\chi^{(3)}$ values of ZnSe were similar to the results obtained in Ref. 35. We can see that the nonlinear susceptibilities of these polymers are as high as 10^{-10} esu, which are as much as those of nitrogen-containing polymers.[7,11,36–38] The large nonlinearity may be mainly originated from the high-electron delocalization between the rigid structure of the fluorene ring and the imine nitrogen of triazole ring. PFTB exhibits the strongest nonlinearity among them, ascribed to the best π-electronic conjugation and coplanarity among fluorene rings, triazole rings, and benzene rings. PFTMB shows better nonlinearity compared with PFTBU, which may be attributed to the n-π conjugation effect between benzene groups and methylene and the better coplanarity.

Table III. Nonlinear Optical Properties of PFTB, PFTMB, PFTBU, and ZnSe

	Nonlinear optical properties		
Polymers	β ($\times 10^{-10}$ m/W)	n_2 ($\times 10^{-16}$ m^2 /W)	χ ($\times 10^{-10}$ esu)
PFTB	1.70	1.50	3.66
PFTMB	1.60	−0.80	1.96
PFTBU	0.67	−0.50	1.22
ZnSe	2.35,[a] 2.442[b]	−0.40	2.75,[a] 2.57[b]

[a] Performed by open and close aperture Z-scan technique in this article.
[b] From Ref. 35.

CONCLUSIONS

In this work, three NLO fluorene-based poly(triazole)s were designed and control preparation was achieved through the click chemistry reactions. All the polymers demonstrated high thermal stability and good third-order nonlinearity owing to the introduction of triazole linked chain. In poly(triazole)s, the rigid conjugated linked chain between triazole and chromophore can effectively enhance the NLO properties of resultant polymers. Their thermal stability can be greatly improved with the suitable linked groups in the triazole polymers. This work would provide a new strategy for the molecular design of NLO materials with large optical nonlinearity and good thermal stability.

ACKNOWLEDGMENTS

The work was financially supported by the National Natural Science Fund of China (grant nos. 21171034, 51073031, and 21271040), Shanghai Youth Natural Science Foundation (12ZR1440100), "Chen Guang" project supported by Shanghai

Municipal Education Commission and Shanghai Education Development Foundation (12CG37), and the Fundamental Research Funds for the Central Universities (12D10603).

REFERENCES

1. Su, X. Y.; Guang, S. Y.; Li, C. W.; Xu, H. Y.; Liu, X. Y.; Wang, X.; Song, Y. L. *Macromolecules* **2010**, *43*, 2840.
2. Su, X. Y.; Guang, S. Y.; Xu, H. Y.; Liu, X. Y.; Li, S.; Wang, X.; Deng, Y.; Wang, P. *Macromolecules* **2009**, *42*, 8969.
3. Bhawalkar, J. D.; He, G. S.; Park, C. K.; Zhao, C. F.; Ruland, G.; Prasad, P. N. *Opt. Commun.* **1996**, *124*, 33.
4. Bouit, P. A.; Wetzel, G.; Berginc, G.; Loiseaux, B.; Toupet, L.; Feneyrou, P.; Bretonniere, Y.; Kamada, K.; Maury, O.; Andraud, C. *Chem. Mater.* **2007**, *19*, 5325.
5. Zhan, X. W.; Liu, Y. Q.; Zhu, D. B.; Liu, X. C.; Xu, G.; Ye, P. X. *Chem. Phys. Lett.* **2002**, *362*, 165.
6. Yin, S.; Xu, H.; Su, X.; Wu, L.; Song, Y.; Tang, B. Z. *Dyes Pigments* **2007**, *75*, 675.
7. Yin, S. C.; Xu, H. Y.; Su, X. Y.; Gao, Y. C.; Song, Y. L.; Lam, J. W. Y.; Tang, B. Z.; Shi, W. F. *Polymer* **2005**, *46*, 10592.
8. Espa, D.; Pilia, L.; Marchio, L.; Mercuri, M. L.; Serpe, A.; Barsella, A.; Fort, A.; Dalgleish, S. J.; Robertson, N.; Deplano, P. *Inorg. Chem.* **2011**, *50*, 2058.
9. Sui, B.; Zhao, W.; Ma, G. H.; Okamura, T.; Fan, J.; Li, Y. Z.; Tang, S. H.; Sun, W. Y.; Ueyama, N. *J. Mater. Chem.* **2004**, *14*, 1631.
10. Guang, S.; Yin, S.; Xu, H.; Zhu, W.; Gao, Y.; Song, Y. *Dyes Pigments* **2007**, *73*, 285.
11. Su, X.; Xu, H.; Guo, Q.; Shi, G.; Yang, J.; Song, Y.; Liu, X. *J. Polym. Sci. Part A Polym. Chem.* **2008**, *46*, 4529.
12. Xu, H.; Yin, S.; Zhu, W.; Song, Y.; Tang, B. *Polymer* **2006**, *47*, 6986.
13. Yin, S. C.; Xu, H. Y.; Fang, M.; Shi, W. F.; Gao, Y. C.; Song, Y. L. *Macromol. Chem. Phys.* **2005**, *206*, 1549.
14. Yin, S. C.; Xu, H. Y.; Shi, W. F.; Gao, Y. C.; Song, Y. L.; Tang, B. Z. *Dyes Pigments* **2006**, *71*, 138.
15. Yin, S. C.; Xu, H. Y.; Su, X. Y.; Li, G.; Song, Y. L.; Lam, J.; Tang, B. Z. *J. Polym. Sci. Part A Polym. Chem.* **2006**, *44*, 2346.
16. Yin, S.; Xu, H.; Shi, W.; Bao, L.; Gao, Y.; Song, Y.; Tang, B. Z. *Dyes Pigments* **2007**, *72*, 119.
17. Wang, X.; Guan, S.; Xu, H.; Su, X.; Zhu, X.; Li, C. *J. Polym. Sci. Part A: Polym. Chem.* **2010**, *48*, 1406.
18. Wang, X.; Guang, S.; Xu, H.; Su, X.; Yang, J.; Song, Y.; Lin, N.; Liu, X. *J. Mater. Chem.* **2008**, *18*, 4204.
19. Wang, X.; Wu, J.; Xu, H.; Wang, P.; Tang, B. Z. *J. Polym. Sci. Part A: Polym. Chem.* **2008**, *46*, 2072.
20. Chu, C.; Liu, R. *Chem. Soc. Rev.* **2011**, *40*, 2177.
21. Michinobu, T. *Chem. Soc. Rev.* **2011**, *40*, 2306.
22. Moses, J. E.; Moorhouse, A. D. *Chem. Soc. Rev.* **2007**, *36*, 1249.
23. Juricek, M.; Felici, M.; Contreras-Carballada, P.; Lauko, J.; Bou, S. R.; Kouwer, P. H. J.; Brouwer, A. M.; Rowan, A. E. *J. Mater. Chem.* **2011**, *21*, 2104.
24. Parent, M.; Mongin, O.; Kamada, K.; Katan, C.; Blanchard-Desce, M. *Chem. Commun.* **2005**, 2029.
25. Feng, Y.; Jia, Y.; Guang, S.; Xu, H. *J. Appl. Polym. Sci.* **2010**, *115*, 2212.
26. Lin, N. B.; Liu, X. Y.; Diao, Y. Y.; Xu, H. Y.; Chen, C. Y.; Ouyang, X. H.; Yang, H. Z.; Ji, W. *Adv. Funct. Mater.* **2012**, *22*, 361.
27. Sheik-Bahae, M.; Said, A. A.; Wei, T.-H.; Hagan, D. J.; Stryland, E. W. V. *IEEE J. Quantum Electron.* **1990**, *26*, 760.
28. Zhu, Y. K.; Guang, S. Y.; Su, X. Y.; Xu, H. Y.; Xu, D. Y. *Dyes Pigments* **2013**, *97*, 175.
29. Qin, A. J.; Jim, C. K. W.; Lu, W. X.; Lam, J. W. Y.; Haussler, M.; Dong, Y. Q.; Sung, H. H. Y.; Williams, I. D.; Wong, G. K. L.; Tang, B. Z. *Macromolecules* **2007**, *40*, 2308.
30. Yan, Z. Q.; Guang, S. Y.; Su, X. Y.; Xu, H. Y. *J. Phys. Chem. C.* **2012**, *116*, 8894.
31. Yan, Z. Q.; Guang, S. Y.; Xu, H. Y.; Su, X. Y.; Ji, X. L.; Liu, X. Y. *RSC Adv.* **2013**, *3*, 8021.
32. Yan, Z. Q.; Xu, H. Y.; Guang, S. Y.; Zhao, X.; Fan, W. L.; Liu, X. Y. *Adv. Funct. Mater.* **2012**, *22*, 345.
33. Zhang, C.; Song, Y. L.; Wang, X.; Kuhn, F. E.; Wang, Y. X.; Xue, Y.; Xin, X. Q. *J. Mater. Chem.* **2003**, *13*, 571.
34. Hou, H. W.; Ang, H. G.; Ang, S. G.; Fan, Y. T.; Low, M. K. M.; Ji, W.; Lee Y. W. *Phys. Chem. Chem. Phys.* **1999**, *1*, 3145.
35. Gaura, A.; Sharmab, D. K.; Ahlawatc, D. S.; Singhd, N. *Solid State Commun.* **2007**, *141*, 445.
36. Zhan, X. W.; Liu, Y. Q.; Zhu, D. B.; Xu, G.; Liu, X. C.; Ye, P. X. *Appl. Phys. A* **2003**, *77*, 375.
37. Yan, J. W. J.; Zhu, H.; Zhang, X.; Sun, D.; Hu, Y.; Li, F.; Sun, M. *Opt. Commun.* **1995**, *116*, 425.
38. Yu, L. P.; Dalton, L. R. *Macromolecules* **1990**, *23*, 3439.